



ISSN: 0067-2904

Distinction of Two Zero-Spaced Iron Pipes in GPR Radargram for Engineering Problems

Jassim M. Thabit^{1*}, Hawkar B. Bakir²

¹Department of Geology, College of Science, Baghdad University, Baghdad, Iraq

²Department of Petroleum Engineering, Faculty of Engineering, Koya University, Koysinjaq, Iraq

Abstract

The researchers have tried to focus on how to determine the number of pipes that are present in one obtained hyperbola in radargram profile. Ground Penetration Radar (GPR) survey was performed to distinguish between two zero-spaced iron pipes in radargram. The field work was carried out by constructing artificial rectangular models with dimensions of length, width, and depth equal to 10.0, 1.0, 0.65 meter respectively that filled with dry clastic mixture deposit, three twin sets of air filled iron pipes of 15.24 cm (6 inch) diameter were buried horizontally and vertically inside the mixture at different distances together. Visual and Numerical interpretation were chosen to get the best results. In the visual interpretation, the amplitude variations show that the height of the positive peaks increases with the increase of the space distance between the buried pipes. Numerical interpretation appeared that the decrease in the width of the bands means an increase of the space between the pipes. The second part of the numerical analysis comprises measuring the amplitude value variation, among the signal forms; relying on the value of amplitude in each hyperbola the distinction process becomes quite easy. Depending on the variations in amplitude, the identification and discrimination of two closely spaced underground pipes will be feasible. The big values refer to highly spaced pipes while the low values denote the slightly spaced pipes. It is worth mentioning that the lowest value indicates the amplitude of only one buried iron pipe.

Keywords: GPR, Iron Pipes, Engineering Problems, Horizontal and Vertical Resolution

تمييز مسافة التباعد بين الأنابيب الحديدية في التسجيلات الجيورادارية للأغراض الهندسية

جاسم محمد ثابت^{1*}، هاوکار بابیر بکر²

¹قسم علوم الأرض، كلية العلوم، جامعة بغداد، بغداد، العراق.

²قسم هندسة النفط، كلية الهندسة، جامعة كويّة، كويسنجق، العراق

الخلاصة:

حاول الباحثان التركيز على كيفية تحديد عدد الأنابيب التي تظهر في القطع الزائد للمقطع الجانبي الجيوراداري. تم إجراء المسح الجيوراداري للتمييز بين اثنين من الأنابيب الحديدية المتباعدة بمسافات مختلفة. لذلك تم تنفيذ العمل الحقل من خلال بناء نماذج مستطيلة ذات أبعاد (10.0 × 1.0 × 0.65) متراً مكعباً تحتوي على مزيج لرواسب فتاتية، وتم دفن ثلاث مجموعات ثنائية من أنابيب الحديد بقطر 15.24 سنتيمتر (6) أنجاً أفقياً وعمودياً داخل المزيج وعلى مسافات مختلفة. وقد تم اختيار التفسير البصري والعدي للحصول على أفضل النتائج. في التفسير البصري، اختلافات السعة يشير إلى أن ارتفاع القمم الموجبة في السعة يزداد مع زيادة المسافة بين الأنابيب المدفونة. التفسير العدي أظهر أن النقصان في العرض إلى القطع الزائد (Hyperbola) يعني زيادة المسافة بين الأنابيب. الجزء الثاني من التحليل العدي يتألف من قياس

*Email:jassimthabit@yahoo.com

التباين في قيمة السعة بين أشكال الأشارة، والاعتماد على قيمة السعة في كل قطع زائد تصبح عملية التمييز سهلة جدا. اعتمادا على الاختلافات في السعة، يكون من الممكن تحديد وتمييز اثنين من الأنابيب المدفونة تحت سطح الأرض و متابعة بمسافة معينة. القيم الكبيرة تشير إلى مسافة تباعد كبيرة بين الأنابيب، في حين أن القيم المنخفضة تشير إلى مسافة قليلة بين الأنابيب. ومن الجدير بالذكر أن القيم الأقل تشير إلى أن السعة هي لأنبوب حديدي واحد.

Introduction:

Ground Penetrating Radar (GPR) is a geophysical and Remote Sensing, non-destructive method that has been developed over the past thirty years for high resolution and subsurface investigations. GPR produces high frequency pulsed electromagnetic waves (generally 10 MHz to 2.0 GHz) and usually operate in the VHF-UHF region of the electromagnetic spectrum that travel through the ground until these waves meet geological targets or different objects then they reflect to the surface [1-3].

The possibility of detecting and locating underground or buried objects remotely has fascinated mankind for centuries. A single technique which could render the ground and its contents clearly visible is potentially so attractive that considerable scientific and engineering effort has gone into devising suitable methods of exploration. As yet, no single method has been found to provide a complete answer, but seismic, electrical resistivity, induced polarization, gravity surveying, magnetic surveying, and electromagnetic methods have all proved useful. Ground penetrating Radar, Ground probing or surface penetrating radar has been found to be an especially attractive option [4, 5].

The application of Ground Penetrating Radar in engineering, mining, and environmental geology studies is well documented and highly effective [6-11].

The new development of GPR techniques, acquisition, and processing used multi frequency antenna, complex 3D datasets, and computer programs to increase data collection and resolution over larger areas [12-17].

Discovering the number of zero-spaced and shape of the underground pipelines that have occupied small subsurface area is still regarded as one of the big problems that are relevant to shortages in shallow depth investigating geophysical method. Radargram hyperbolas are considered as one of the diagnostic features to identify the number of subsurface pipelines through the number of its peaks. In the literature, there are still few published works dealing with the automatic detection of patterns associated with buried objects [18].

This research is an attempt to focus on how to determine the number of pipes that are present in one obtained hyperbola. In order to explain the ways that relate to solving this issue with high resolution.

Data collection:

The field work was started after constructing artificial rectangular models with dimension of length, width, and depth (10.0, 1.0, 0.65) meter respectively that filled with dry clastic mixture deposit, three twin sets of air filled iron pipes of 15.24 cm in diameter were buried horizontally and vertically at depth equals to 0.65 m (65 cm) inside the mixture at different distances together, as shown in Figure-1 and -2. The instrument comprised a portable RIS One and RIS Plus GPR System Figure-3. Common-offset profiling mode of survey under the control of IDS factory setting parameters ($\epsilon_r = 15$, range = 128 ns, sample/scan = 384, and velocity = 10 cm/ns) were used.



Figure 1 – Lined Horizontal and vertical iron pipes inside the dry mixture clastic deposit model.

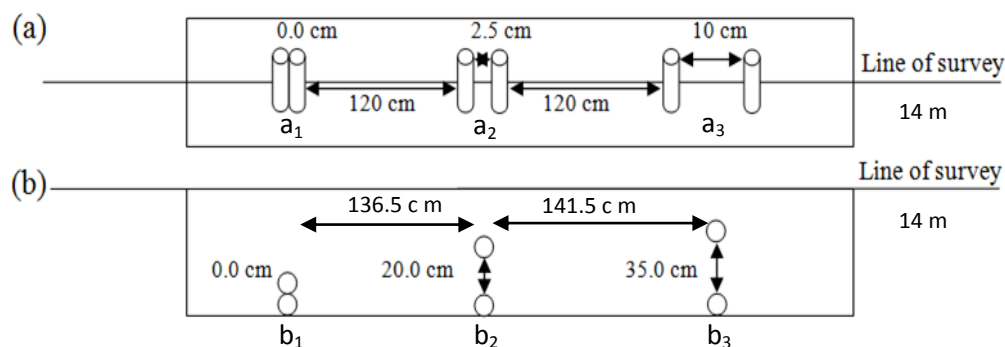


Figure 2- Shows (a) the top view of horizontal arranging of the three twin sets of empty iron pipes (a_1 , a_2 , and a_3) within the dry mixture model (b) the side view of vertical arranging of the three twin sets of empty iron pipes (b_1 , b_2 , and b_3) within the dry mixture.

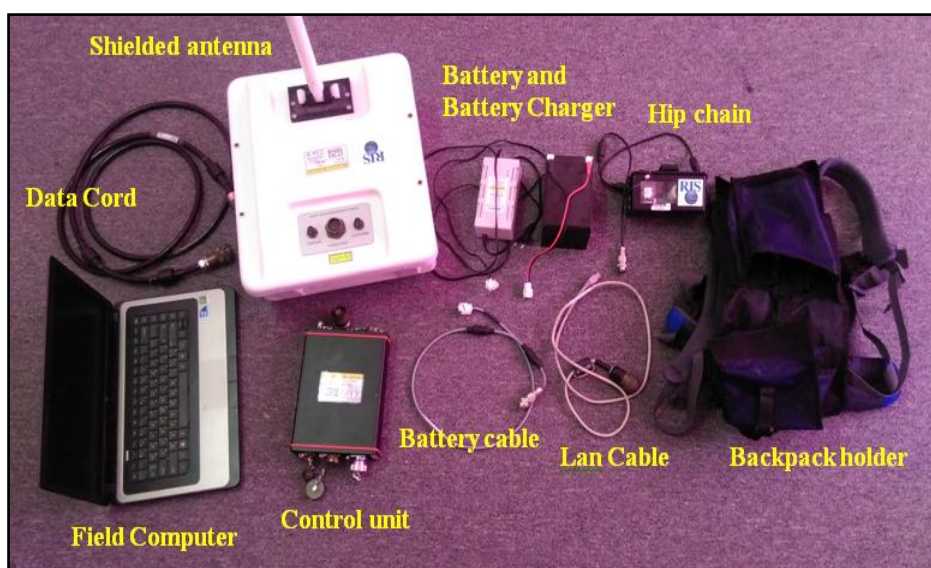


Figure 3 - Shows RIS One and RIS Plus GPR System.

Data analysis and Interpretation:

The analysis and processing of the collected field data were performed by using GRED.exe and Reflex 2D Quick software [19, 20]. These programs can omit the bad data that distorts the radargrams, helps to describe the hyperbola's peak shape and shows the existed form of current traces or signals. To get the best results both visual and numerical interpretation were chosen as follows:

Visual Interpretation:

Visual analysis and interpretation comprise an explanation of the hyperbola's peak shape and demonstrate the existed form of current traces and signals Figures-4,-5,- 6, and -7 a-d. Figure-4 refers to a radargram of one iron pipe within the dry mixture, the hyperbola's peak shape is completely curved downward and there is no any clear sign of existing flat peak surface. Figure 5 indicates three hyperbolas which have wide peak shapes as compared with Figure-4. In Figure-5 surface flattening is starting from left to right (a_1 to a_3) depending on the increase of the distance between the pipes. Moreover, appearances of hyperbolas peak splitting can obviously be seen now in the middle (a_2) and the right (a_3) of hyperbolas which belong to 2.5 and 10.0 cm space between the iron pipes. Figure-6 refers to vertical arranging of iron pipes. It can easily be distinguished the middle (b_2) and right (b_3) vertically set and arranged pipes while the left-hand pipe (b_1) is still facing the same problem that exists in the horizontal arranging of pipes. In order to know the exact number of zero vertically spaced pipes, the amplitude value measuring is the best option, see Figure-8.

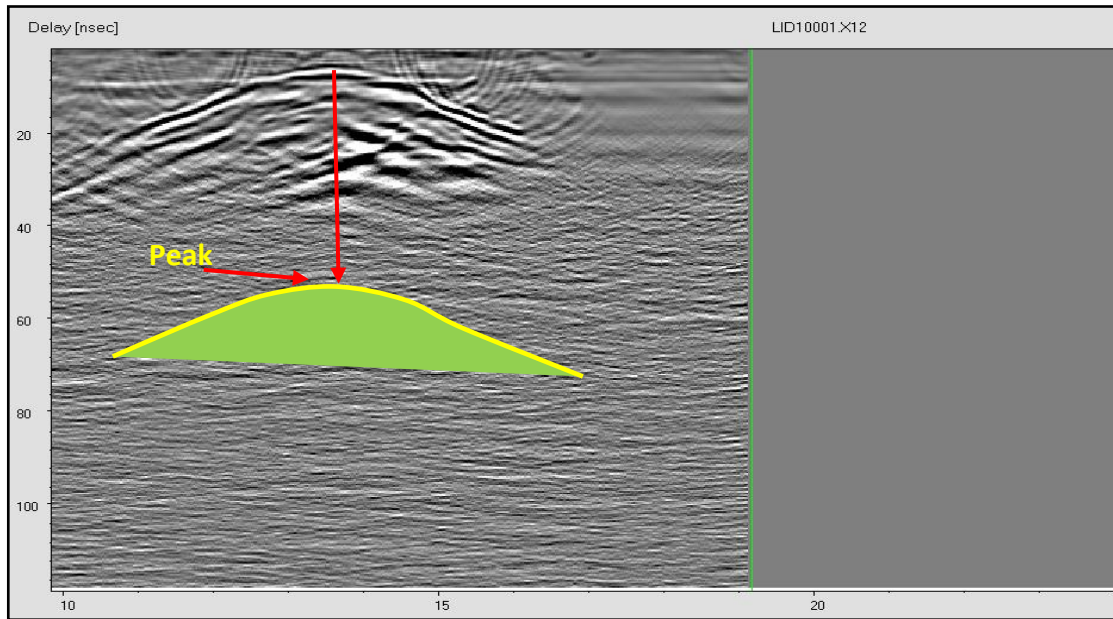


Figure 4- shows raw radargram of mixture model (one iron pipe within mixture), horizontal resolution test, using factory setting parameters ($\epsilon_r = 15$, range = 128 ns, sample/scan = 384, and velocity = 10 cm/ns).

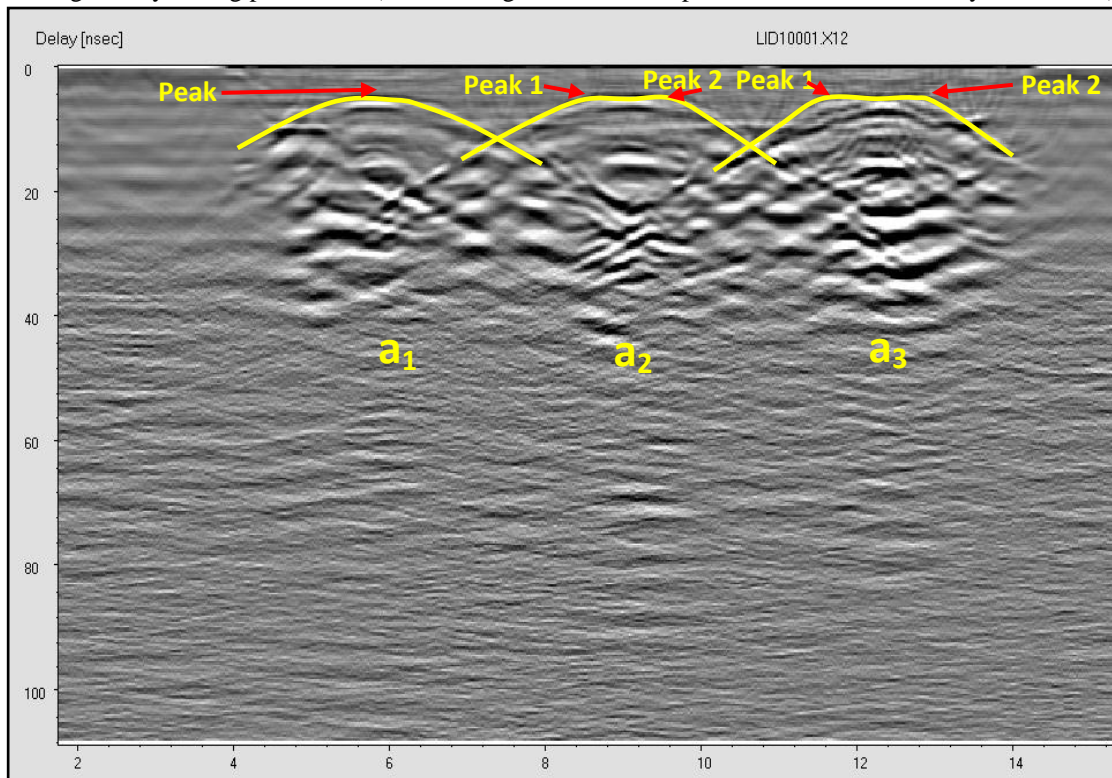


Figure 5- shows raw radargram of mixture model (two iron pipes within mixture), horizontal resolution test, factory setting parameters ($\epsilon_r = 15$, range = 128 ns, sample/scan = 384, and velocity = 10 cm/ns).

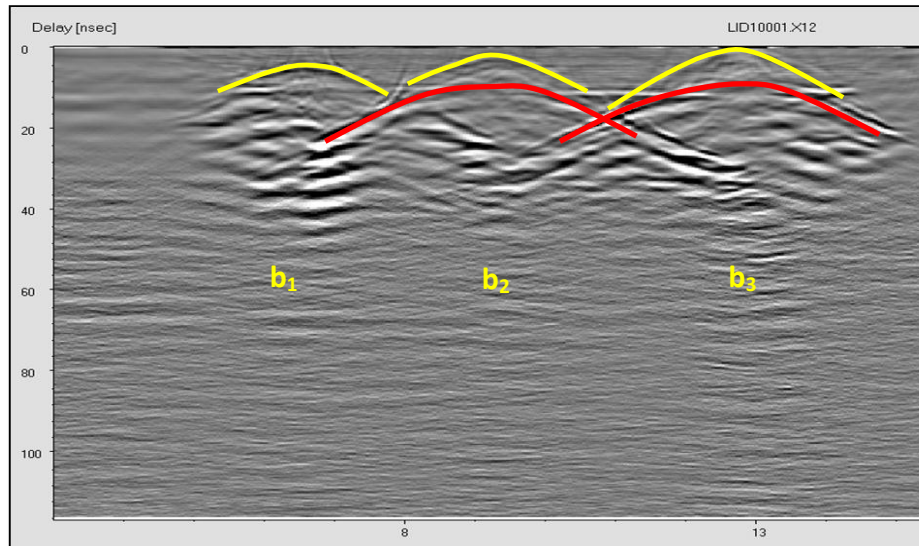


Figure 6 - shows raw radargram of mixture model (two iron pipes within mixture), vertical resolution test, using factory setting parameters ($\epsilon_r = 15$, range = 128 ns, sample/scan = 384, and velocity = 10 cm/ns).

Figure-8 shows the amplitude variation is very clear; the amplitude value of the radargram that includes one iron pipe is (5171) and the radargram that contains two vertically zero-spaced iron pipes is (9620). Figures-7a and d refer to a signal form that has one iron pipe Figure-7a and signal form that has more than one pipe. Figures-7b, c, d show a big difference between the signal forms especially in the length or height of the pipe's positive peaks. The height of the positive peaks increases with the increase of the space distance between the buried pipes. So, the amplitudes show a direct relationship with the spacing between two pipes.

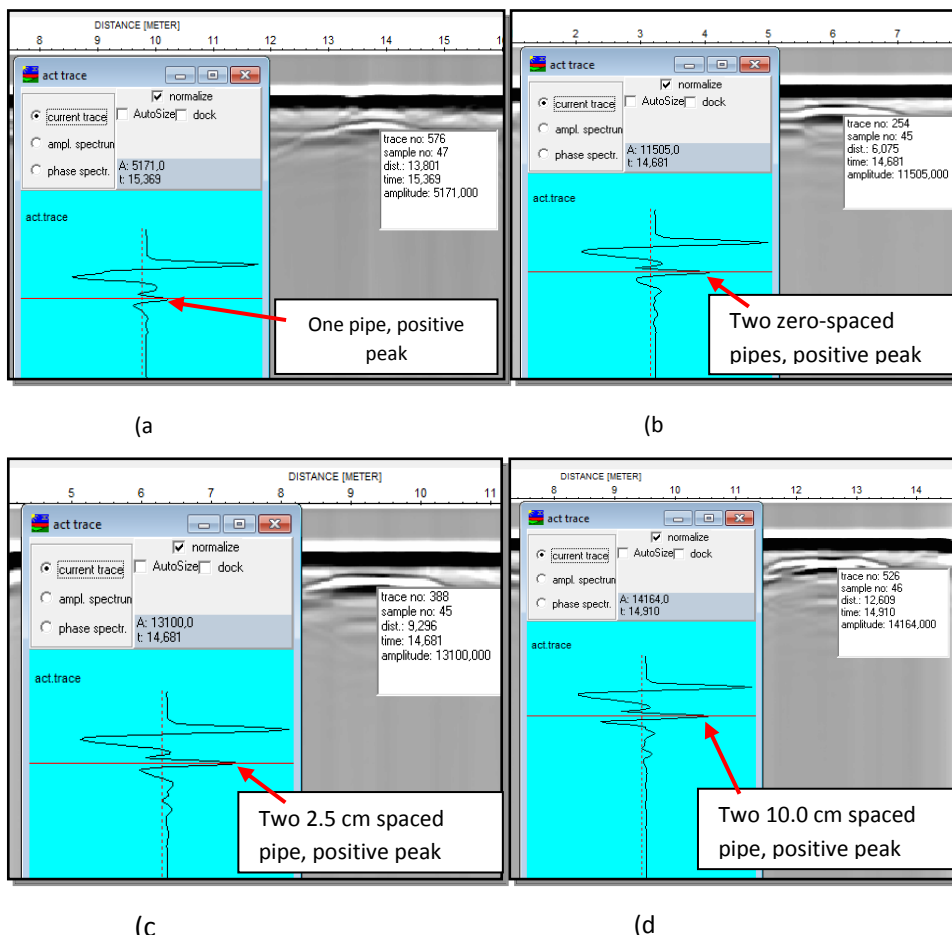


Figure 7(a-d) - shows comparison between the signal form of one alone iron pipe and two horizontally arranged iron pipes at different distanced within mixture together.

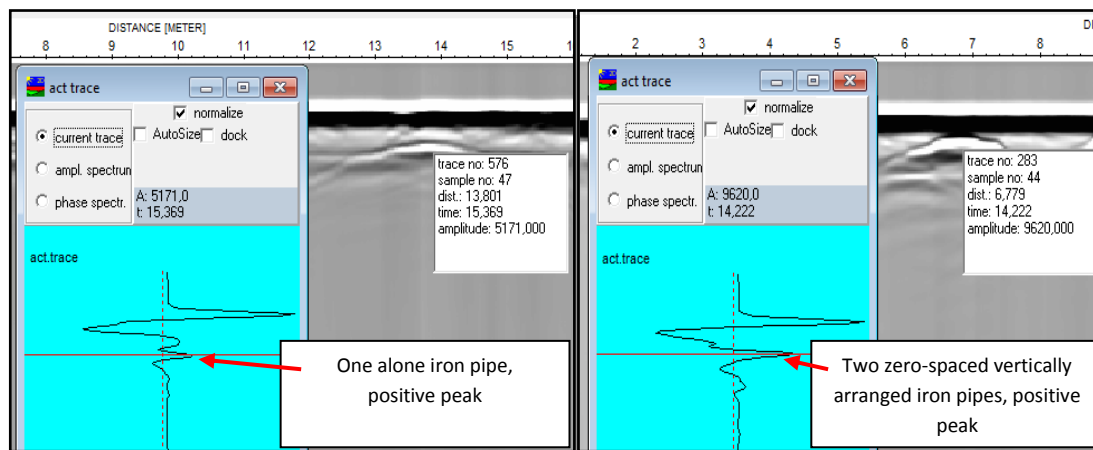


Figure 8 - shows comparison between the signal form of one alone iron pipe and two zero-spaced vertically arranged iron pipes within mixture together.

Numerical Interpretation:

In order to demonstrate and verify the fact of visual interpretation and to confirm the results, there is another method which is called numerical interpretation that can help this part of the study.

Figure-9 shows to the amount of horizontal space between the buried pipes. This space appears as clear dark-white-dark bands located inside the middle part of each hyperbola and determined by two vertical yellow lines. Through measuring the width of the bands the researchers could find the amount of separation between the buried pipes on the radargrams that leads to identify the presence of more than one pipe inside the subsurface materials, see Table-1.

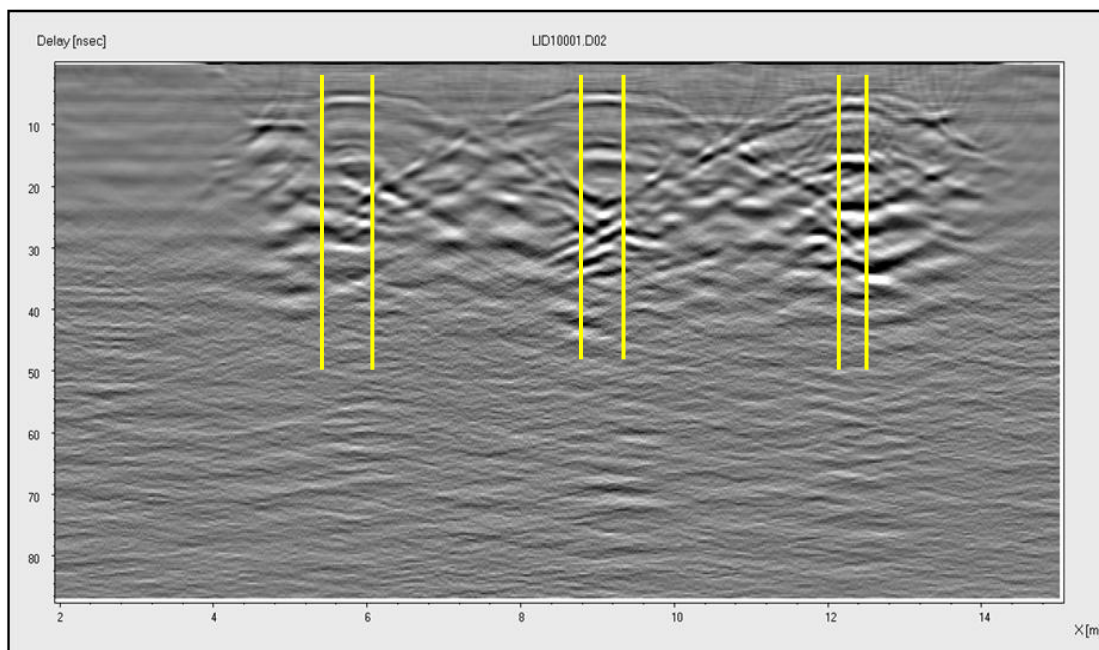


Figure 9 - shows appeared width between the hyperbola’s peaks of buried pipes, raw radargram of dry mixture model (two iron pipes within mixture), horizontal resolution test, factory setting parameters ($\epsilon_r = 15$, range = 128 ns, sample/scan = 384, and velocity = 10 cm/ns).

Table 1 - shows the width of appeared dark-white-dark band on the radargrams that relates to the actual space between the pipes.

Hyperbola position	Band width (m)
Left	0.6
Middle	0.5
Right	0.4

Over all, decrease in the width of the bands means increase of the space between the pipes, it means inverse relationship between them. The second part of the numerical analysis comprises measuring the amplitude value variation. Figure-7 shows the signal forms; relying on the value of amplitude in each hyperbola the distinction process become quite easy, see Table-2. Depending on these amplitude value variation from figures (a to d), the identification and discrimination of two closely spaced underground pipes will be feasible. The big values refer to highly spaced pipes while the low values denote the slightly spaced pipes. It is worth mentioning that the lowest value indicates the amplitude of only one buried iron pipe.

Table 2- shows the amplitude value variation of the current signals that belong to the iron pipe within dry mixture model.

Hyperbola in Figure (7)	Horizontal arranging of twin sets	Amplitude value
a	One iron pipe	5171
b	(a ₁)	11505
c	(a ₂)	13100
d	(a ₃)	14164

Conclusion:

Radargram of one iron pipe within dry mixture shows hyperbola's peak shape is completely curved downward, and there is no any clear sign of existing flat peak surface. Radargram of mixture model (two iron pipes within mixture) shows surface flattening is starting from left to right (a₁ to a₃) depending on the increase of the distance between the pipes. Moreover, appearances of hyperbolas peak splitting can obviously be seen now in the middle and the right of hyperbolas (a₂ and a₃) which belong to 2.5 and 10.0 centimeters space between the iron pipes. While in the vertical arranging of twin sets of iron pipes, it can easily be distinguished the middle and right (b₂ and b₃) vertically set and arranged pipes, while the left hand pipe (b₁) is still facing the same problem that exists in the horizontal arranging of pipes. The comparison between the signal forms of two vertically arranged iron pipes within mixture together shows a big difference between the signal forms especially in the length or height of the pipe's positive peaks. The height of the positive peaks increases with the increase of the space distance between the buried pipes, In addition, the amplitude variations show that the height of the positive peaks increases with the increase of the space distance between the buried pipes, it means a direct relationship between them.

Numerical interpretation appeared that the decrease in the width of the bands means increase of the space between the pipes (inverse relationship). The second part of the numerical analysis comprises measuring the amplitude value variation, among the signal forms; relying on the value of amplitude in each hyperbola the distinction process become quite easy. Depending on the variations in amplitude, the identification and discrimination of two closely spaced underground pipes will be feasible. The big values of amplitude refer to highly spaced pipes while the low values denote the slightly spaced pipes. It is worth mentioning that the lowest value indicates the amplitude of only one buried iron pipe. It is concluded that the results could help the civil engineers to find the underground utilities before planning to excavate the proposed area for building and constructing new projects.

Acknowledgments:

We would like to thank Mr. Muhammad Faqe, the Director of Koya water directorate to supply requirements of the field work. We would like to thank Dr. Abdulqadir G. Anuar, the head of geotechnical engineering department in the faculty of engineering, Koya University. Our thanks to the Engineer Mr. Botan A. Muhammed, the director of Koya University's Engineering Directorate for providing an area inside the Koya University campus to carry our field work.

References:

1. Ulriksen, C. P. F. **1982**. Application of impulse radar to civil engineering: Unpublished Ph.D. Thesis, Department of Engineering Geology, University of Technology, Lund, Sweden, p:175.
2. Davis, J. L. and Annan, A. P. **1989**. Ground penetrating radar for high-resolution aping of soil and rock stratigraphy, *Geophysical Prospecting*, 37, pp: 531–551.
3. Daniels, D. J. **1996**. Surface penetrating radar—IEE Radar, Sonar, Navigation and Ionics Series 6: London, The Institute of Electrical Engineers, p:320.
4. Daniels, D.J. **2004**. *Ground Penetrating Radar*, Second Edition, The Institution of Electrical Engineers, London, p:761.

5. Cheng, N., Tang, H.C. and Chan, C. **2013**. Identification and positioning of underground utilities using ground penetrating radar (GPR). *Journal of Sustain. Environ. Res.*, 23, pp: 141-152.
6. Ulricksen, C.P. **1982**. Application of impulse radar to civil engineering, Ph.D. Thesis, Lund University of Technology, Lund, Sweden, p:175.
7. Pilon, J.A. **1992**. Ground penetrating radar, Geological Survey of Canada, Paper 90-4, p:241.
8. Grandjean, G. and Gourry, J.C. **1996**. GPR data processing for 3d fracture mapping in a marble quarry (Thassos, Greece), *Journal of Applied Geophysics*, 36(1), pp: 19–30.
9. Arcone, S.A., Lawson, D.E., Delaney, A.J., Strasser, J.C. and Strasser, J.D. **1998**. Ground penetrating radar reflection profiling of groundwater and bedrock in an area of discontinuous permafrost, *Geophysics*, 63(5), pp: 1573-1584.
10. Jack, R. and Jackson, P. **1999**. Imaging attributes of railway track formation and ballast using ground probing radar, *NDT & E International*, 32(8), pp: 457- 462.
11. Bhuiyan, A., and Nath, B. **2006**. Anti-personnel mine detection and classification using GPR image, Proceedings of the International conference on Pattern recognition, 2, pp: 1082-1085.
12. Grasmueck M., Weger R. and Horstmeyer H. **2005**. Full-resolution 3-D GPR imaging. *Geophysics*, 70(1), pp:K12–K19.
13. Linford, N., Linford, P., Martin, L. and Payne, A. **2009**. Stepped frequency GPR survey with a multi-element array antenna: results from field application on archaeological sites, 8th International Conference on Archaeological Prospection, Paris, pp: 317-319.
14. Leckebusch., J. **2009**. Test and data processing of a stepped frequency GPR array, 8th International Conference on Archaeological Prospection, Paris, pp: 305-307.
15. Conyers, L.B. **2013**. *Ground-penetrating Radar for Archaeology* .3rd ed. Rowman and Littlefield Publishers, Alta Mira Press, Latham, Maryland.
16. Goodman, D., and Piro, S. **2013**. *GPR remote sensing in archaeology*. Springer-Verlag, Berlin, Heidelberg, p:233.
17. Linford, N. **2014**. Rapid processing of GPR time slices for data visualization during field acquisition, Proceedings of the 15th International Conference on Ground Penetrating Radar (eds S. Lambot, A. Giannopoulos, L. Pajewski, F. André, E. Slob and C. Craeye, 731-735. Square Brussels Meeting Centre, Brussels, Belgium: Université Catholique de Louvain.
18. He, X., Zhu, Z., liu, Q., and Lu, G. **2009**. *Review of GPR Rebar Detection*. PIERS Proceedings, Beijing, China, pp: 805-813.
19. Gred Software. **2008**. The software for GPR data elaboration. Version 02.01.008, Italy, p:136.
20. Reflex 2D Quick. **2014**. The software for GPR data processing and interpretation. Version 2.5. Sandmeier geophysical software, p:61.